Inelastic scattering of α particles on light nuclei at $P_\alpha = 7.0$ GeV/c

J. Banaigs,[a] J. Berger,[a] P. Berthet,[b] G. Bizard,[c] M. Boivin,[d] M. De Sanctis,[e] J. Duflo,[a]
F. L. Fabbri,[e] R. Frascaria,[b] L. Goldzahl,[a] P. Picozza,[e] F. Plouin,[a] and L. Satta[e]

[a]*IN2P3, ER54, Laboratoire National Saturne, Saclay, France*
[b]*Institut de Physique Nucleaire, Orsay, France*
[c]*Laboratoire de Physique Corpusculaire, ISMRA, Université de Caen, Caen, France*
[d]*Laboratoire National Saturne, Saclay, France*
[e]*Istituto Nazionale di Fisica Nucleare, Laboratori Nazionali di Frascati, Frascati, Italy*

(Received 21 July 1986)

The inclusive inelastic scattering of α particles on ^{2}H, ^{3}He, and ^{4}He has been measured at 7.0 GeV/c incident momentum, between 2° and 15° in the laboratory. The momentum spectra of the recoiling α particles are richly structured, suggesting that scattering takes place, at least partially, on nuclear substructures. The differential cross sections for the three reactions show a diffractive behavior comparable to that of the corresponding elastic processes.

I. INTRODUCTION

Experimental investigation of the hadron—light nucleus scattering is a powerful tool with which to obtain information on the light nuclei structure, nucleon-nucleon interaction, and reaction mechanisms. As a matter of fact, the small number of nucleons involved permits a detailed description of data by theoretical models which are still easy to handle.[1]

Experimental and theoretical efforts up to now have concentrated on the elastic scattering. However, it should be noted that a more direct access to the nuclear wave function is given by the study of the nuclear fragmentation in the momentum transfer region up to the opening of π production channels. A full experimental exploitation of this process requires a detailed knowledge of the final states, which can be obtained by using large angle detectors ($\sim 4\pi$), typically bubble chambers.[2]

A somewhat different approach to the inelastic diffusion can be reached through inclusive experiments, by measurements of angular and momentum distributions of the recoiling projectile.[3,4] Then, the data can be analyzed either by using inelastic sum rules that involve only the nucleus ground state properties, or by models taking into account detailed microscopic description of the scattering process.[4-7]

In this paper we present the measurement of the inclusive cross section for the reactions

$$\alpha\,^2\text{H} \rightarrow \alpha X , \tag{1}$$

$$\alpha\,^3\text{He} \rightarrow \alpha X , \tag{2}$$

$$\alpha\,^4\text{He} \rightarrow \alpha X \tag{3}$$

performed at 7.0 GeV/c incident alpha momentum at the Saturne II synchrotron at Saclay. It is worth noting that the data have been collected for the different nuclei in almost the same momentum transfer interval, so that any theory has to work consistently for the three processes. The data concerning the elastic scattering have already

been published.[8]

We stress that, to the best of our knowledge, no other set of measurements exists in the intermediate energy domain, exploring the so called quasielastic region simultaneously for three nuclei up to transferred momenta of ~ 4 GeV^2/c^2.

II. EXPERIMENTAL SETUP

The experimental setup, shown in Fig. 1, consisted of an α beam extracted from the Saturne synchrotron at Saclay, a set of liquid targets which could be put alternatively in the beam, and the double focusing magnetic spectrometer SPES IV. The α beam, with an intensity of 10^{11} particles per pulse (one pulse every 2.5 sec, 500 msec long) and a momentum of 7.0 GeV/c had, at the target, a Gaussian profile with an 11 mm and a 3 mm full width at half maximum (FWHM) in the vertical and in the horizontal plane, respectively, visualized by wire chambers along the beam line. The relative intensity monitoring was provided by three scintillation counter telescopes, two of them viewing a thin plastic target placed downstream the extraction point, and one looking at the target at a fixed angle of 70°. The monitors' stability was within 1%. The absolute intensity value was derived by activation of a thin carbon target through the reaction ^{12}C(α,X)^{11}C with a $\sim 5\%$ precision.

The ^{4}He, ^{3}He, and ^{2}H targets were contained in different titanium cylinders 3.8 cm long with walls of 28 μm, housed together with an equal empty cylinder, in a vacuum chamber with two internal aluminum windows 6 μm thick, and one external window of 50 μm havar material.

The SPES IV spectrometer is composed of four analyzing identical magnetic dipoles, six focalizing quadrupoles, and two sextupoles. The diffused α particles accepted by the spectrometer were first focused on seven 1 mm thin scintillation counters placed in the intermediate image, and then defocused on a hodoscope at the final image.

Four plastic scintillator planes, 1 cm thick, comprise the hodoscope; the first, divided in 44 strips 1.4 cm wide placed side by side, provides $\Delta p/p \simeq 0.2\%$. The other planes each consist of one of seven scintillation counters, 1 cm thick. The total momentum acceptance was of $\sim 8\%$. The momentum analyzed particles were identified by time of flight between the two images on a basis of 16 meters, and by energy loss in the counters. The contaminating particles were limited to less than 1% of the secondary α beam.

At the spectrometer entrance, 3.2 m from the center of the target, a lead collimator defined a solid angle $\Delta\Omega = 2.47 \times 10^{-4}$ sr. The angular region explored by the spectrometer ranges between 0° and 28° with an angular precision of $\sim 0.1°$. The angle setting is obtained by moving the target along an axis perpendicular to the beam line and then deflecting the incident beam onto its center. Wire chambers monitored the whole operation. The nominal angle is related to the central trajectory, corresponding to the central counter of the first scintillator plane at
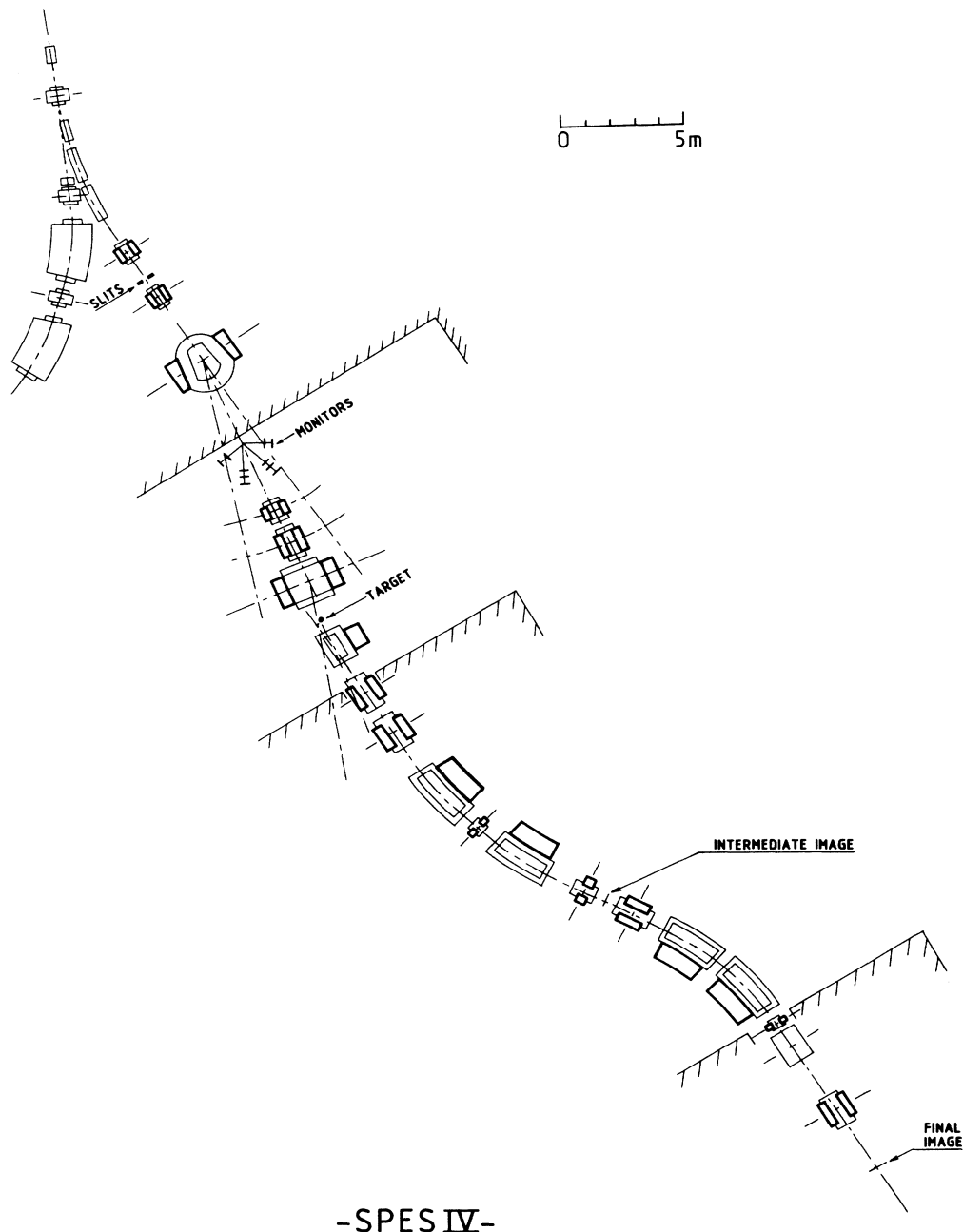

-SPES IV-

FIG. 1. The SPES IV spectrometer. The time of flight basis for particle identification between the counters placed at the intermediate and final image is 16 m.
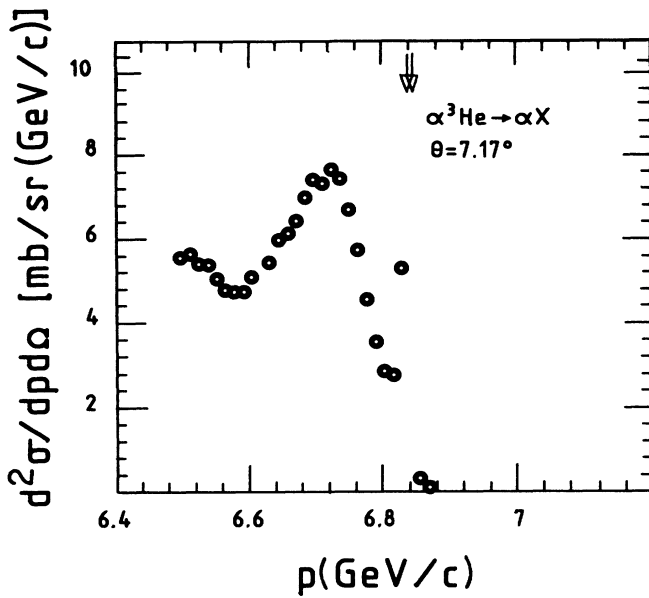
FIG. 2. A typical momentum spectrum of the recoiling α for the α^3He$\rightarrow\alpha$X reaction. The arrows indicate the kinematical position of the elastic peak and the threshold for the target nucleus fragmentation. This spectrum does not cover the whole quasielastic region up to the pion production threshold.

the final image. A linear relation gives the displacement of each lateral counter from this nominal value, with a maximum of 0.14°.

III. DATA TAKING

Data have been taken in about 300 runs, alternating the different liquid targets and the empty one on the beam. For each angular setting the momentum distribution of
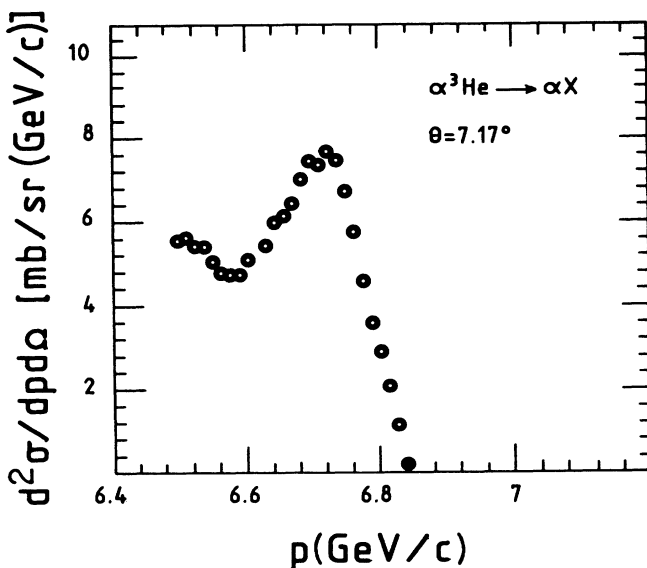
the detected α was explored from the elastic peak to the one pion production.

Data have been reduced to cross sections in different steps. Empty target contribution was normalized to the same incident α flux and subtracted; in addition, corrections for nuclear absorption effects and individual counter efficiency were applied.

As an example, in Fig. 2 $d^2\sigma/d\Omega\,dp$ is shown as a

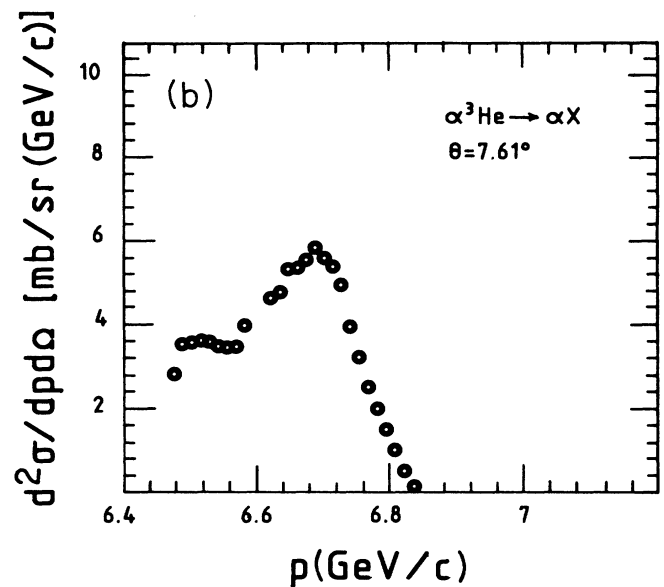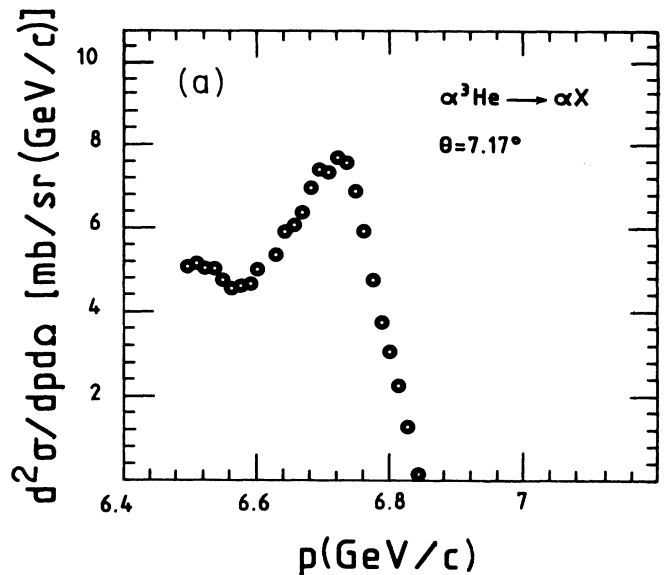FIG. 3. The same spectrum of Fig. 2, after the subtraction of the elastic peak.

FIG. 4. The effect of the angular correction described in the text on the spectrum of Fig. 3 is shown in panel (a). The net effect of the correction is to lower the experimental points at the smaller momenta and to raise those at higher momenta. Panel (b) shows the auxiliary spectrum employed for the correction. The two spectra are less than 0.5° apart.
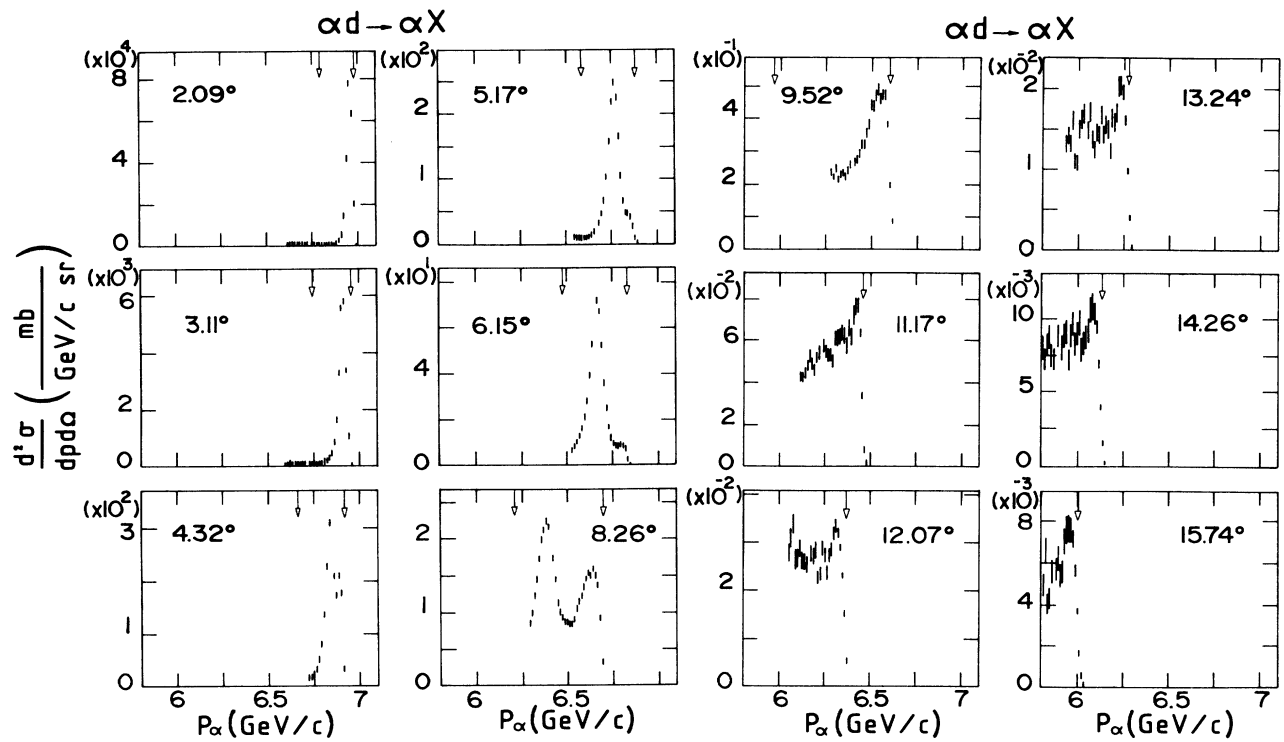
FIG. 5. Twelve $\alpha\,^2\mathrm{H}\to\alpha X$ momentum spectra. The arrows indicate the nuclear fragmentation and π production thresholds. The angular evolution of the subprocesses constituting the quasielastic scattering is rather clear.
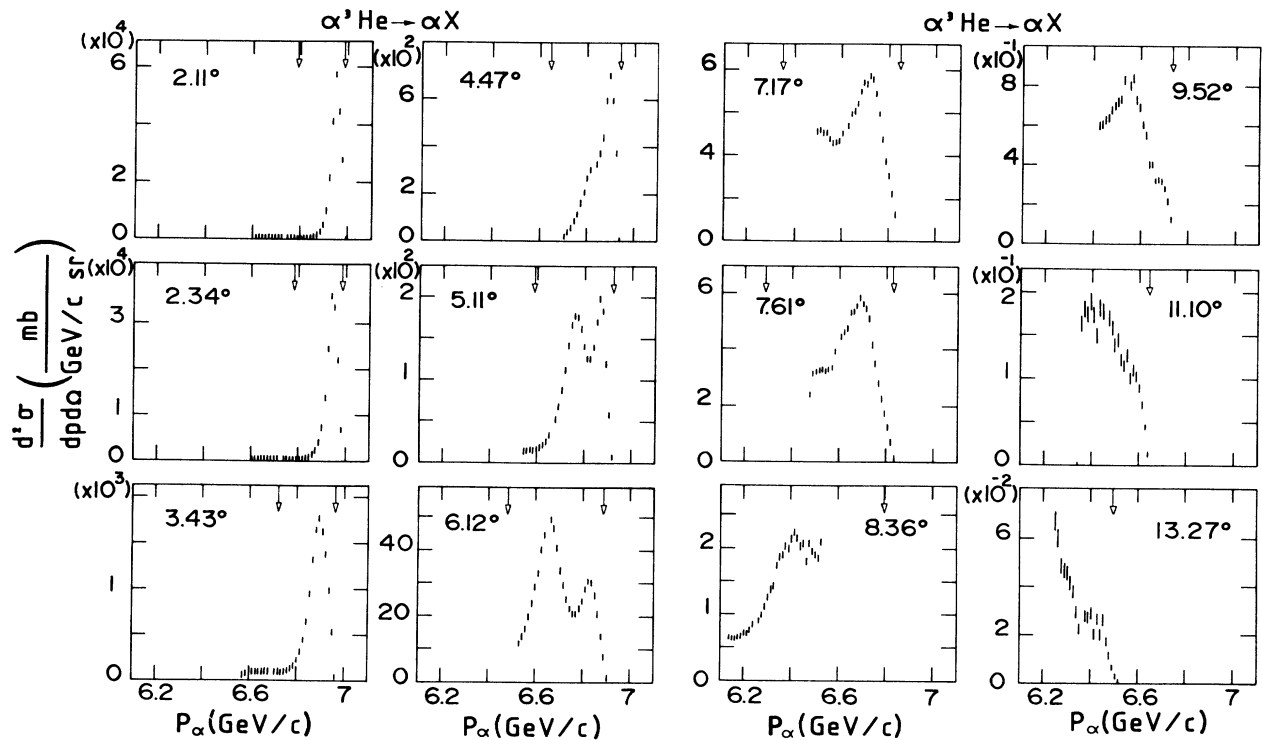

FIG. 6. The same momentum spectra of Fig. 5 for the $\alpha\,^3\mathrm{He}\to\alpha X$ reaction.
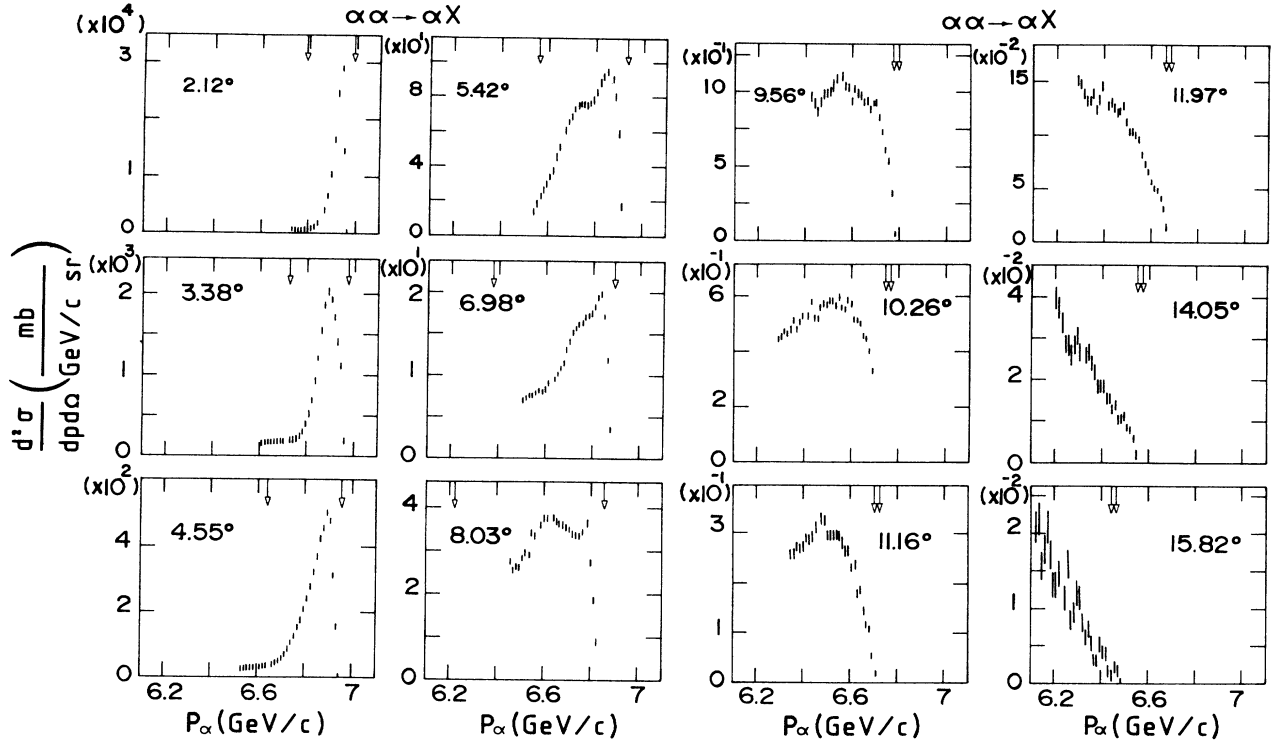
FIG. 7. The same momentum spectra of Fig. 5 for the $\alpha\,^4\mathrm{He}\rightarrow\alpha X$. The difference between the structures appearing in the quasi-elastic region is less pronounced with respect to the lighter nuclei.

function of the laboratory momentum for the $\alpha\,^3\mathrm{He}$ reaction. Beginning from the right hand side, the arrows show the position of the elastic peak and the inelastic threshold. The opening of the π production channel at this particular angle is at 6.35 GeV/c. The different processes involved clearly stand out; furthermore, the quasielastic region presents a structured behavior.

The first step of the analysis consisted of the evaluation and subtraction of the elastic peak. Due to the collimator acceptance and the spectrometer finite resolution, the elastic peak and the threshold of the inelastic process partially overlap. The separation has been obtained by taking into account the characteristics of the spectrometer and the kinematical constraints. In Fig. 3 the same spectrum of Fig. 2 is shown, after the subtraction of the elastic scattering.

Since in the same spectrum different momenta are related to slightly different angles, as noted in Sec. II, we developed an interpolation method to reduce each point of the inelastic spectrum to a fixed angle corresponding to the central momentum. Points in different spectra having almost the same momenta and a close angle have been used. This correction is always small. Figure 4 shows the spectrum of Fig. 3, with all the points related to the same angle, together with the auxiliary spectrum used for the interpolation.

IV. EXPERIMENTAL RESULTS

In Figs. 5, 6, and 7 the cross sections for the quasielastic scattering of α on $^2\mathrm{H}$, $^3\mathrm{He}$, and $^4\mathrm{He}$ are presented at 12

different angles. The kinematical positions of the elastic scattering and the nuclear fragmentation and pion production threshold are indicated by arrows. Where the momenta corresponding to elastic scattering and the quasielastic threshold are very close, only the last one is indicated.

Different structures appear in the kinematical position of the elastic scattering of α particles on nucleon clusters in the target nucleus, broadened by Fermi motion. All these structures exhibit a pronounced angular dependence. For momenta below the pion production threshold, at several angles, the cross section shows an additional structure whose peak value is about 50 times smaller than the quasielastic one. This enhancement corresponds to the coherent one pion production on a single nucleon, already observed in the dp and αp interactions.[9] Figures 8—10 show a few experimental spectra on a logarithmic scale, plotted in three dimensions. The angular evolution of the structures is quite evident.

To compare the angular dependence of the quasielastic cross section with the elastic scattering, $d^2\sigma/d\Omega\,dp$ has been integrated over the momentum of the detected α at fixed angle. To avoid arbitrary extrapolation of data, only the spectra extending to at least the pion production threshold have been used. The coherent pion production has not been subtracted, since its contribution to the integral is negligible. The $d\sigma/d\Omega$ obtained for the three nuclei, shown in Figs. 11—13, together with the corresponding elastic cross sections, span 6—7 orders of magnitude. The general trend follows the elastic one, with less
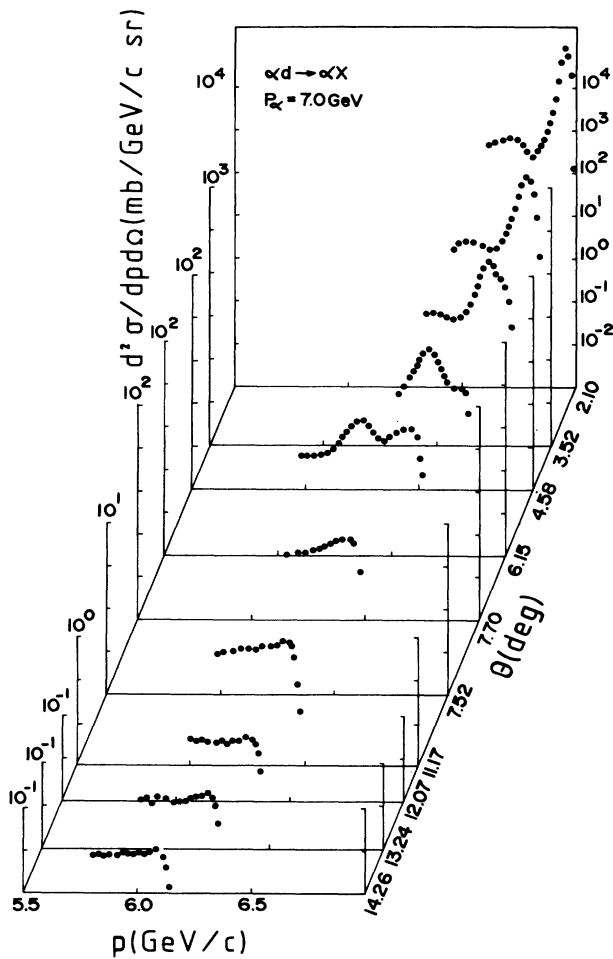
FIG. 8. Momentum spectra for the $\alpha\,^2\mathrm{H}\rightarrow\alpha X$ reaction, plotted on a logarithmic scale in three dimensions, to underline the global angular evolution of the quasielastic scattering.

pronounced dips. The higher value of the inelastic cross section at large angles with respect to the elastic reflects the richness of the multiple scattering contributions on the different clusters.

The full collection of data are available from the Physics Auxiliary Publication Service of AIP.[12] Table I gives an index of the measurements performed.

V. MODELS AND CONCLUSIONS

Theoretical models for inelastic scattering at medium energy are very few, perhaps because of the lack of experimental data. An interpretation of the $\alpha\alpha$ inclusive scattering in the framework of the model of independent nucleons has been proposed by Fujita and Hüfner,[5] evaluating analytically the Glauber-Matthiae series[11] for the inclusive hadron-nucleus scattering. Their calculation gives for our previous $\alpha\alpha$ data an absolute and parameter-free prediction of the integrated cross section

$d\sigma/dq^2$, but fails to reproduce the shape. Krimm $et\ al.$[6] improved this calculation by including quantum mechanical corrections and using a more sophisticated parametrization of the αp cross sections.

A further approach to the interpretation of the same data has been proposed by Malecki $et\ al.$, based on the inelastic sum rule in the framework of multiple scattering theory.[7] All these models reproduce reasonably the quasielastic angular distribution.

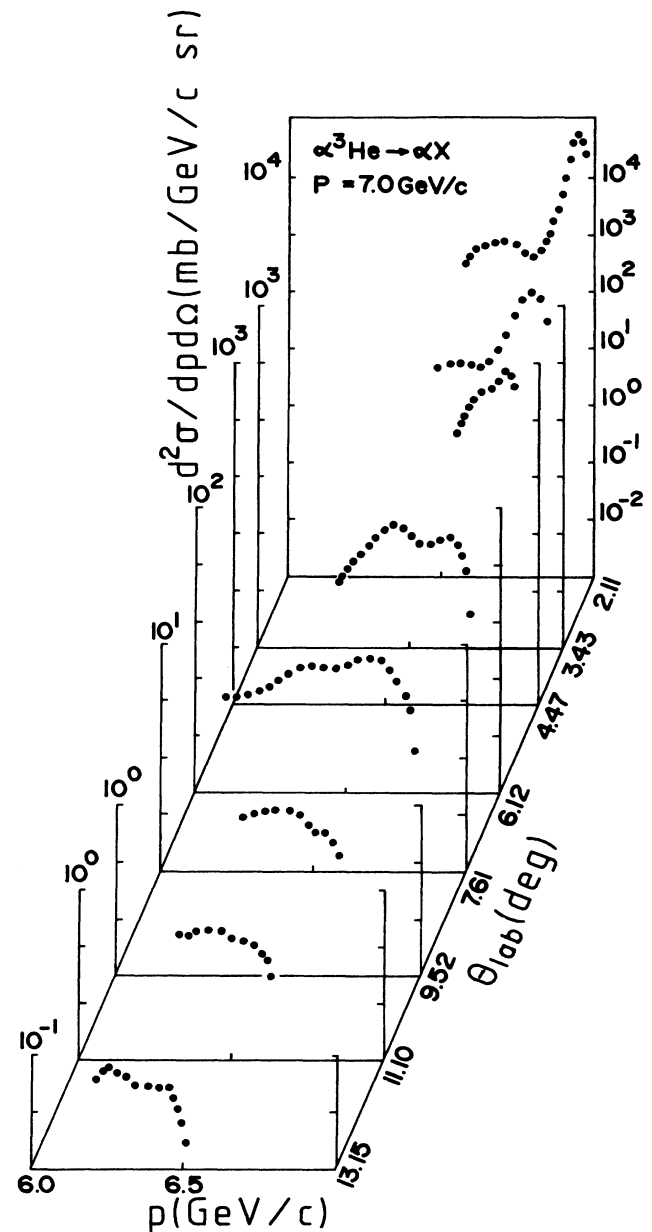A phenomenological analysis of the first $\alpha\alpha$ data has

FIG. 9. Same as Fig. 8 for the $\alpha\,^3\mathrm{He}\rightarrow\alpha X$ reaction.

TABLE I. Summary of the measurement of the inclusive $\alpha\,^2H\rightarrow\alpha X$, $\alpha\,^3He\rightarrow\alpha X$, and $\alpha\alpha\rightarrow\alpha X$ reactions.

θ (deg)	p_{min} (GeV/c)	p_{max} (GeV/c)	θ (deg)	p_{min} (GeV/c)	p_{max} (GeV/c)
	$\alpha\,^2H\rightarrow\alpha X$			$\alpha\,^3He\rightarrow\alpha X$	
2.09	6.615	6.992	4.83	6.565	6.926
2.34	6.602	6.980	5.06	6.555	6.929
2.43	6.716	6.991	5.11	6.547	6.920
2.89	6.601	6.991	5.19	6.553	6.914
3.11	6.591	6.967	5.34	6.537	6.911
3.52	6.573	6.949	5.40	6.533	6.906
3.96	6.735	6.940	6.12	6.531	6.903
4.32	6.722	6.941	6.69	6.233	6.702
4.36	6.654	6.920	7.17	6.498	6.842
4.55	6.706	6.925	7.61	6.475	6.832
4.58	6.532	6.918	7.70	6.206	6.674
4.95	6.567	6.900	8.36	6.139	6.601
4.99	6.558	6.905	9.52	6.426	6.727
5.15	6.556	6.903	11.10	6.358	6.733
5.17	6.548	6.908	13.27	6.251	6.506
5.41	6.534	6.894			
5.45	6.539	6.872			
6.15	6.532	6.838		$\alpha\alpha\rightarrow\alpha X$	
6.69	6.235	6.704			
6.92	6.504	6.848	2.11	6.614	6.991
7.30	6.499	6.764	2.11	6.733	6.996
7.70	6.476	6.767	2.34	6.602	6.966
7.70	6.207	6.676	2.43	6.715	6.963
8.12	6.455	6.718	3.09	6.600	6.963
8.25	5.963	6.412	3.38	6.590	6.953
8.26	6.293	6.703	3.63	6.572	6.949
8.36	6.141	6.602	4.12	6.734	6.953
9.12	6.453	6.637	4.33	6.721	6.940
9.52	6.281	6.614	4.55	6.531	6.930
9.99	6.293	6.626	4.88	6.566	6.927
10.24	5.963	6.412	5.09	6.558	6.918
10.26	5.632	6.056	5.16	6.555	6.929
11.08	6.171	6.498	5.25	6.547	6.921
11.17	6.117	6.478	5.38	6.533	6.920
11.47	6.101	6.500	5.42	6.538	6.925
12.07	6.052	6.458	6.10	6.531	6.904
13.24	5.929	6.291	6.69	6.234	6.703
14.26	5.798	6.152	6.98	6.503	6.914
15.74	5.765	6.035	7.70	6.206	6.675
			7.62	6.475	6.846
			8.03	6.454	6.849
			8.25	5.962	6.411
	$\alpha\,^3He\rightarrow\alpha X$		8.26	6.291	6.765
			8.36	6.140	6.601
2.11	6.613	6.991	8.36	6.729	6.798
3.34	6.601	6.978	8.94	6.453	6.781
2.43	6.715	6.989	9.56	6.427	6.793
3.11	6.600	6.962	10.26	6.290	6.738
3.17	6.590	6.966	10.26	5.631	6.055
3.43	6.572	6.961	11.15	6.346	6.708
3.95	6.733	6.953	11.97	6.290	6.713
4.26	6.520	6.945	13.16	6.251	6.658
4.35	6.720	6.939	14.05	6.205	6.609
4.47	6.704	6.937	14.26	5.897	6.341
4.54	6.530	6.930	15.82	6.122	6.471

FIG. 10. Same as Fig. 8 for the $\alpha\,^4$He$\rightarrow\alpha$X reaction.

FIG. 12. Same as Fig. 11 for the $\alpha\,^3$He$\rightarrow\alpha$X reaction.

been reported in the original experimental paper, which gives a fit of the experimental spectra.[4] It was based on the incoherent addition of elastic collisions of the α projectile on the different substructures in the target α nucleus. This interpretation is applied to the new data by one of the authors of the present work.[10] The assumptions used in the first analysis are expanded to the different light targets and for all the angles measured. Discrepancies appear and they are interpreted as arising from double scattering.

The main trends of the first experimental spectra are also reproduced by the calculations of Krimm et al.[6] The present data on different light nuclei and covering a large angular and momentum interval bring new constraints on all theoretical interpretations of nucleus-nucleus collisions.
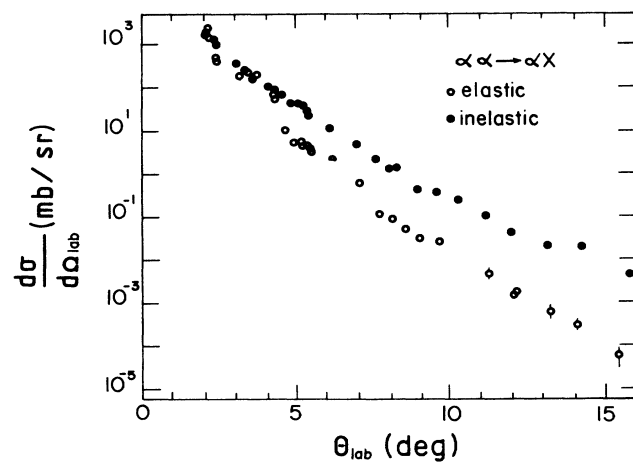
FIG. 11. Solid circles: angular distribution of the inelastic $\alpha\,^2$H$\rightarrow\alpha$X reaction. Open circles: angular distribution of αd$\rightarrow\alpha$d. The points are plotted vs the laboratory angle, instead of the usual four-momentum transfer. As a matter of fact, the inelastic spectra, whose integration gives the solid circles, do not have a definite momentum transfer. For the comparison with the elastic scattering, the measured laboratory angle seems a more natural variable.

FIG. 13. Same as Fig. 11 for the $\alpha\,^4$He$\rightarrow\alpha$X reaction. The structures appearing in the elastic angular distribution are less pronounced for the inelastic reaction.

[1]V. Franco and Yichun Yin, Phys. Rev. Lett. **55**, 1059 (1985).

[2]A. V. Blinov *et al.*, J. Phys. G **11**, 683 (1985); Institute of Theoretical and Experimental Physics, Moscow, Report No. 60, 1985.

[3]V. G. Ableev *et al.*, Acta Phys. Polon. B **16**, 913 (1985).

[4]J. Duflo *et al.*, Nucl. Phys. **A356**, 427 (1981).

[5]T. Fujita and J. Hüfner, Phys. Lett. **87B**, 327 (1979).

[6]H. Krimm *et al.*, Nucl. Phys. **A367**, 333 (1981).

[7]A. Małecki *et al.*, Phys. Lett. **136B**, 319 (1984).

[8]L. Satta *et al.*, Phys. Lett. **139B**, 263 (1984).

[9]F. L. Fabbri *et al.*, Nucl. Phys. **A338**, 429 (1980); R. Baldini-Celio *et al.*, *ibid.* **A379**, 477 (1982); J. Banaigs *et al.*, *ibid.* **A445**, 737 (1985).

[10]J. Duflo, Phys. Rev. C (to be published).

[11]R. J. Glauber and G. Matthiae, Nucl. Phys. **B21**, 135 (1970).

[12]See AIP document no. PAPS PRVCA-35-1416-101 for 101 pages of tabulated measured cross sections. Order by PAPS number and journal reference from the American Institute of Physics, Physics Auxiliary Publication Service, 335 East 45th Street, New York, N.Y. 10017. The prepaid price is $3.00 for microfiche or $15.65 for photocopies. Airmail additional.